Distinct metabolomic profiling of serum samples from high fat diet-induced insulin resistant mice

Manendra Singh Tomar [a], Aditya Sharma[b], Fabrizio Araniti [c], Ankit Pateriya [a], Ashutosh Shrivastava [a*], Akhilesh Kumar Tamrakar [b*]

[a] Centre for Advance Research, Faculty of Medicine, King George's Medical University, Lucknow-226003, India.

[b] Division of Biochemistry and Structural Biology, CSIR-Central Drug Research Institute, Lucknow, 226031, India.

[c] Dipartimento di Scienze Agrarie e Ambientali—Produzione, Territorio, Agroenergia, Università degli Studi di Milano, Via Celoria 2, 20133 Milano, Italy.

Correspondence:

Dr. Ashutosh Shrivastava, Ph.D.

Additional Professor

Center for Advance Research, Faculty of Medicine, King George's Medical University, Lucknow - 226003, Uttar Pradesh, India.

E-mail: ashutoshshrivastava@kgmcindia.edu

Dr. Akhilesh Kumar Tamrakar, Ph.D.

Senior Principal Scientist

Division of Biochemistry and Structural Biology, CSIR-Central Drug Research Institute, Lucknow, 226031, India.

Email: akhilesh_tamrakar@cdri.res.in

Abstract

High-fat diet (HFD) induced obesity is associated with elevated risk of insulin resistance (IR) that may precede the onset of type 2 diabetes mellitus and associated metabolic complications. Being a heterogeneous metabolic condition, it is pertinent to understand the metabolites and metabolic pathways that are altered during development and progression of IR towards T2DM. Serum samples were collected from C57BL/6J mice fed with HFD or chow diet (CD) for 16 weeks. Collected samples were analysed using Gas Chromatography-Tandem Mass Spectrometry (GC-MS/MS). The identified raw metabolites data were evaluated using a combination of univariate and multivariate statistical methods. Mice fed with HFD had glucose and insulin intolerance associated with impairment of insulin signalling in key metabolic tissues. From the GC-MS/MS analysis of serum samples, a total of 75 common annotated metabolites were identified between HFD- and CD-fed mice. In the t-test, 22 significantly altered metabolites were identified. Out of these, 16 metabolites were up-accumulated whereas 6 metabolites were down-accumulated. Pathway analysis identified 4 significantly altered metabolic pathways. In particular, primary bile acid biosynthesis and linoleic acid metabolism were upregulated, whereas TCA cycle and pentose and glucuronate interconversion were downregulated in HFD-fed mice in comparison to CD-fed mice. These results show the distinct metabolic profiles associated with the onset of IR that could provide promising metabolic biomarkers of diagnostic and clinical applications.

Keywords: Insulin Resistance, High fat diet, Metabolomics, Gas Chromatography-Tandem Mass Spectrometry**,** Type II Diabetes Mellitus

A regulated nutrient metabolism is a fundamental requisite for growth, development and survival of all the organisms. Physiologically, a coordinated response of multiple metabolic pathways ensures proper functioning and sound physiology.[1] Insulin is the principal acute regulator of nutrient metabolism. Insulin signals through insulin receptors and downstream activation of phosphatidylinositide-3-kinase (PI3K) and Akt regulates the metabolism of carbohydrates, lipids and protein to establish nutrient homeostasis.[2] IR is the condition in which cells are not in a position to respond optimally to the normal level of circulating insulin.[3] IR is the primary risk factor underlying the development and progression of metabolic diseases, including T2DM, non-alcoholic fatty liver disease, cardiovascular disease, etc.[4] The pathophysiology of IR is multivalent, characterized by intricate connections among genetic, metabolic, immune pathways, nutritional, and life style modifications.[5]

Diet is a noticeable element in regulation of the metabolic status of an individual. Precisely, consumption of high fat diet (HFD) and sedentary life style cause obesity.[6] Obesity is a complex metabolic condition characterized by an excessive body fat and lead to increased risk of other diseases, such as T2DM, cardiovascular disease and other metabolic disorders.[7] Obesity has led to a global health care burden due to associated comorbid conditions. It is widely accepted that the increasing prevalence of obesity leads to IR, and caloric excess and a sedentary lifestyle are additive factors determining its manifestations.[8] Although, obesity has been considered as a critical cue leading to metabolic diseases, mechanistic links between these two have not been precisely recognized. Integration of functional genomics, transcriptomics and proteomics have led to a deeper understanding of molecular mechanisms underlining obesity, IR and T2DM.[9] Advent of metabolomics and lipidomics have significantly broadened our understanding of IR in relation to T2DM.[10-11] However, linking obesity to IR using newer metabolomics tool is only beginning to emerge. Several studies have quantified serum metabolites in HFD-fed mice.[12-14] The serum of 8-week-HFD-fed mice

display significantly reduced concentrations of TCA cycle intermediates.[13] Metabolomic changes were found to be associated with Non-alcoholic Fatty Liver Disease (NAFLD) development in a HFD-fed mouse model. In this study, interestingly, at the end of 12 and 16 weeks, metabolites profile predominantly correlated to abnormal bile acid synthesis, oxidative stress, and inflammation, representing hepatic inflammatory infiltration during NAFLD development.[12-14] Although, increasing evidences support the notion that impaired lipid metabolism plays a vital role therein, contribution of other metabolic cues remained under explored.[15-16] Recent advances in metabolic profiling techniques demonstrated high complexity in plasma metabolome.[17] These methods facilitate identification of newer biomarkers associated with obesity, IR and T2DM which may be pertinent to pathophysiology, diagnosis, and therapy for metabolic disorders.

The technology for analyzing metabolome and lipidome raw data set have evolved at a fast pace enabling us to identify novel metabolites and their roles in known metabolic pathways.[18] Consumption of HFD induces inflammation, associated with chronic IR. Saturated fatty acid especially arachidonic acid and palmitic acid are viewed as a pro-inflammatory molecule. Excess of saturated fat can cause inflammation in the metabolic tissues and in hypothalamus as well, disrupting signalling of insulin to regulate nutrient homeostasis.[19-20] With the aim to explore potential metabolic cues modulated during IR development, in the present study, we used an established model of HFD-induced IR for metabolomic analysis. Based on the metabolic alterations, we have also identified the metabolic pathways affected by HFD and linked to the onset of IR.

Materials and Methods:

1. Chemical and reagents: All the solvents and chemicals used in the study were HPLC-grade. Methanol and N-methyl-N-trimethylsilyl trifluoroacetamide with 1% TMCS were

purchased from SRL (Mumbai, India). Chromatography-grade water, methoxamine hydrochloride, and pyridine were procured from Thermo Fisher Scientific (MA, USA). Ribitol used as an internal standard was obtained from Sigma-Aldrich (MO, USA). Alkane standard solution containing C_{10-40}, 50 mg/l in n-hexane was used for measurement of retention indices or performance of GC-MS/MS was purchased from Supelco (Bellefonte, PA, USA). The 60% high fat diet (cat no. # C1090-60) and chow diet (cat no. # C1090-10) were purchased from Altromin (Lage, Germany).

2. Study design:

Male C57BL/6J mice (20±5 g), aged 7-8 weeks available at the National Laboratory Animal Center of the CSIR-Central Drug Research Institute, Lucknow, were used for the study. The work with these animals was approved by the Institutional Animal Ethics Committee (IAEC) of the CSIR-Central Drug Research Institute, Lucknow and was conducted in accordance with the guidelines of the Committee for the purpose of Control and Supervision of Experiments on Animals (CPCSEA) formed by the Government of India. Mice were housed in polypropylene cages in the animal house under standard conditions of temperature 23 ± 2^0C with relative humidity (50–60%), light 300 Lx at floor level along with light and dark cycles of 12h. Animals were provided with standard diet and drinking water *ad libitum*. Mice were divided into two major groups, kept on CD or 60% HFD for 16 weeks with weekly measurement of body weight and fasting blood glucose level. At end of the experiment, intra-peritoneal glucose tolerance tests (GTT) and intra-peritoneal insulin tolerance test (ITT) was performed, as described previously.[21] At the termination of experiment, animals were sacrificed; blood samples were collected, centrifuged to separate serum and stored at -80^0C for further analysis. Tissue samples were excised out and stored in liquid N_2 for further analysis by western blotting, as described previously.[21] Finally, we performed GC-MS/MS

based untargeted metabolomics analysis to identify the metabolic alterations of HFD-fed mice.

3. Glucose/ insulin tolerance test

Animals were subjected to glucose/ insulin tolerance test after 6h fasting. The baseline blood glucose level was monitored at 0 min, followed by an intra-peritoneal injection of glucose (2 g/kg body weight) of insulin (0.75U/kg body weight). The blood glucose levels were again checked at 30 min, 60 min, 90 min, and 120 min post-glucose/ insulin administration.

4. Measurement of insulin levels

Insulin level in serum samples was measured using mouse enzyme linked immunosorbent assay kit (RayBiotech) as per the manufacturer's instructions.

5. Western blot analysis

The Western blot analysis was performed by protein extractions from the metabolic tissues. Tissue samples were lysed in RIPA buffer supplemented with NaOV3 (1 mM), triton X-100 (20%) and protease inhibitor cocktail (1:1000). The lysates were centrifuged (10,000 rpm) for 10 min at 4°C and protein concentration was determined using BCA assay reagent. Lysates with equal amount of protein were heated at 65^0C in Laemmli sample buffer with 10% β-mercaptoethanol. Proteins were resolved by SDS-PAGE and transferred to polyvinylidene difluoride (PVDF) membranes. After blocking, blots were incubated in indicated primary antibody solution for overnight at 4^0C, followed by incubation with appropriate HRP-conjugated secondary antibodies. Immunoblots were developed using enhanced chemiluminescence (ECL, Millipore) reagent. Densitometric quantification of protein bands was performed using National Institute of Health (NIH) Image J software.

6. Extraction and derivatization of metabolites: Before metabolite extraction, 300 µl of chilled methanol was added to 30 µl of serum sample to precipitate protein. Serum metabolites were extracted with a solvent system with methanol: water (3:1; v/v). For primary metabolites extraction, 750 µl of chilled methanol was added to the samples and vortexed for 1 minute. Successively, samples were centrifuged at 8000 rpm for 10 min at 4ºC to remove precipitated proteins and supernatant was collected in separate 2 ml Eppendorf tubes. Again, 250 µl of cold water was added and the samples were vortexed for 2 min, centrifuged at 8000 rpm, and the supernatant was collected. Successively, to the extracted sample 20 µL of ribitol (0.005 mg/mL) were added as internal standard, and the samples were dried. For derivatization, samples were methoximated by adding 20 μl methoxyamine/pyridine (20 mg/ml), vortexed and placed on Eppendorf Thermostat C at 800 rpm for 1 h at 60°C. Successively, methoximated samples were sylilated by adding 80 μl of MSTFA+1% TMCS and incubating them at 60^0C for 30 min.[22]

7. GC-MS/MS based untargeted metabolomic profiling: 1 μl of derivatised samples were injected in a splitless mode by a Triplus 100 autosampler (Thermo Scientific) in Trace 1300 Gas chromatographer equipped with a TSQ 8000 Mass spectrometer (Thermo Scientific). Metabolites were separated on Trace GOLD TG-5MS column (Thermo Scientific) with a diameter of 0.25 mm, thickness of 0.25 µm and length of 30 m at constant flow of Helium at the rate of 1 ml/min. The injector port temperature was set at 200°C, whereas the transfer line and ion source temperature were set at 250°C. The GC programme was as follows: 0-1 min at 50°C, ramping to 100°C at 6°C/min rate, increased up to 200°C at 4°C/min rate and finally to 280°C at 20°C/min rate which was held constant for 3 min. All the samples were run on full scan mode ranging from m/z 60 to 650 Da. The solvent delay was 4 min and total run time for the analysis was 40 min. Derivatized samples were injected in the GC-MS/MS system,

and an alkane standard mixture (C10-C40 all even) was injected at the start and end of sample analysis for retention index (RI) calculation.

8. Raw GC-MS/MS Data Processing: The acquired raw data from GC-MS/MS were pre-processed using MS-Dial version 4.80 for peak picking, alignment, annotation and mass spectral deconvolution. For peak detection and deconvolution, the default MS-Dial parameters were used.[23] Automated annotation of metabolites was achieved using an in-house library built with publicly available MS spectra. The metabolomics standards initiative (MSI) guidelines for metabolite identification for metabolite annotation and assignment of the EI-MS spectra were used.[24] In particular, features were annotated at Level 2 [identification based on the spectral database (match factor >70%)] and Level 3 [identification based on the spectral database (match factor >70%)]. (Putatively characterized compound class based on spectral similarity to known compounds of a chemical class as suggested).

9. Statistical Analysis: Significant alterations among the metabolic profiles of serum samples from CD- and HFD-fed mice were assessed using multivariate and univariate statistical analysis using the open-source software Metaboanalyst 5.0.[25] GC-MS/MS data were normalized by reference feature (ribitol), root transformed and pareto scaled. Normalized data were further analyzed through univariate and multivariate analysis to highlight alterations in metabolites concentration that might help in distinguishing insulin-resistant HFD-fed mice from CD-fed mice. For the identification of statistically meaningful molecules in both groups, univariate statistical measures such as Wilcoxon rank t-test ($p<0.05$) and log 2-fold change were utilized. Volcano plot analysis was carried out using a Fold-change (FC) > 2.0 and FDR corrected P value ≤ 0.05 to reduce significant features detection by focusing on those significant metabolites with a high FC.

Multivariate statistical analysis such as unsupervised principal component analysis (PCA) and the supervised orthogonal partial least square discriminant analysis (OPLS-DA) were used to identify the main metabolites involved in groups separation. The PCA score plot represents the distribution of original data sets and outlier detection. Whereas, OPLS-DA shows metabolite level differences between study groups. These models were used to illustrate the distribution pattern of serum metabolites amongst the studied groups and their efficacy in discriminating insulin resistant HFD-fed mice with CD-fed mice. Features selection with the highest discriminatory power was based on their variable importance in projection (VIP) score > 1. A permutation test with a permutation number set to 20 was developed to evaluate the quality of the resulting statistical model by considering the diagnostic measures R^2 and Q^2, which describe the endpoint variation captured in the regression model, and the variation reproduced in the permutation test. Predictive relevance is considered when R^2 and Q^2 values are higher than 0.5 and $P \leq 0.05$ (Moltu et al., 2014). Pathway analysis was carried out using MetPA, a web-based tool of Metaboanalyst 5.0. A linear support vector machine (SVM) was used to predict the group of metabolites that act as a classifier between insulin-resistant HFD-fed mice and control CD-fed mice by Monte-Carlo cross validation (MCCV) using balanced sub-sampling. All SVM models were compared with variable distribution of metabolites (up to 100). ROC curves were used to evaluate the model, and the feature ranking algorithm built in SVM was used to identify biomarkers.

Results:

1. Establishment of IR Mice Model:

Mice kept on HFD displayed a progressive increase in body mass and fasting blood glucose levels with a marked increase, compared to CD-fed group, observed after 16 weeks of HFD feeding **(Fig. 1a** & **b)**. HFD-fed animals also showed a significant rise in serum insulin levels

after 16 weeks of HFD feeding, compared to CD feeding (**Fig. 1c)**. Assessment of the glucose tolerance showed that HFD feeding in mice induced glucose intolerance which was evidenced at 4 weeks and further exacerbated progressively up to 16 weeks of HFD-feeding. **Fig. 1d** depicts the blood glucose profile of chow- and HFD-fed mice during GTT at 16 weeks; HFD-fed mice were found to be 132.7% ($p<0.001$) more glucose intolerant compared to CD-fed mice (AUC_{120min} of 18088.8 vs. 42097.7 for CD- and HFD-fed mice, respectively, **Fig. 1e**). Moreover, at 16 weeks of HFD-fed mice were found to be 74.3% ($p<0.01$) more insulin intolerant compared to CD-fed mice, as evidenced by ITT (AUC_{120min} of 6235.3 vs. 10870.17 for CD- and HFD-fed mice, respectively, **Fig. 1f** & **g**). The data showed that HFD feeding progressively induces IR and glucose intolerance in mice.

Next, we analysed the activation of insulin signalling in key metabolic tissues viz. skeletal muscle and liver, responsible for regulation of glucose metabolism. Insulin stimulation induces phosphorylation of Akt at Ser-473, required for the further downstream progression of insulin signalling, leading to the regulation of glucose utilization in metabolic tissues.[26] As depicted in **Fig. 1h**, insulin administration caused a profound increase in Akt (Ser-473) phosphorylation in skeletal muscle and liver tissues of CD-fed animals. However, the insulin-stimulated phosphorylation of Akt (Ser-473) was significantly decreased in both skeletal muscle and liver tissues of HFD-fed mice compared to CD-fed animals. Findings indicated the impairment of insulin signaling in skeletal muscle and liver upon HFD feeding in mice. Altogether, our data verified the induction of IR in HFD-fed mice at week 16. Therefore, serum samples from these 16-week HFD-fed mice were subjected to metabolomic analysis, compared to CD-fed mice.

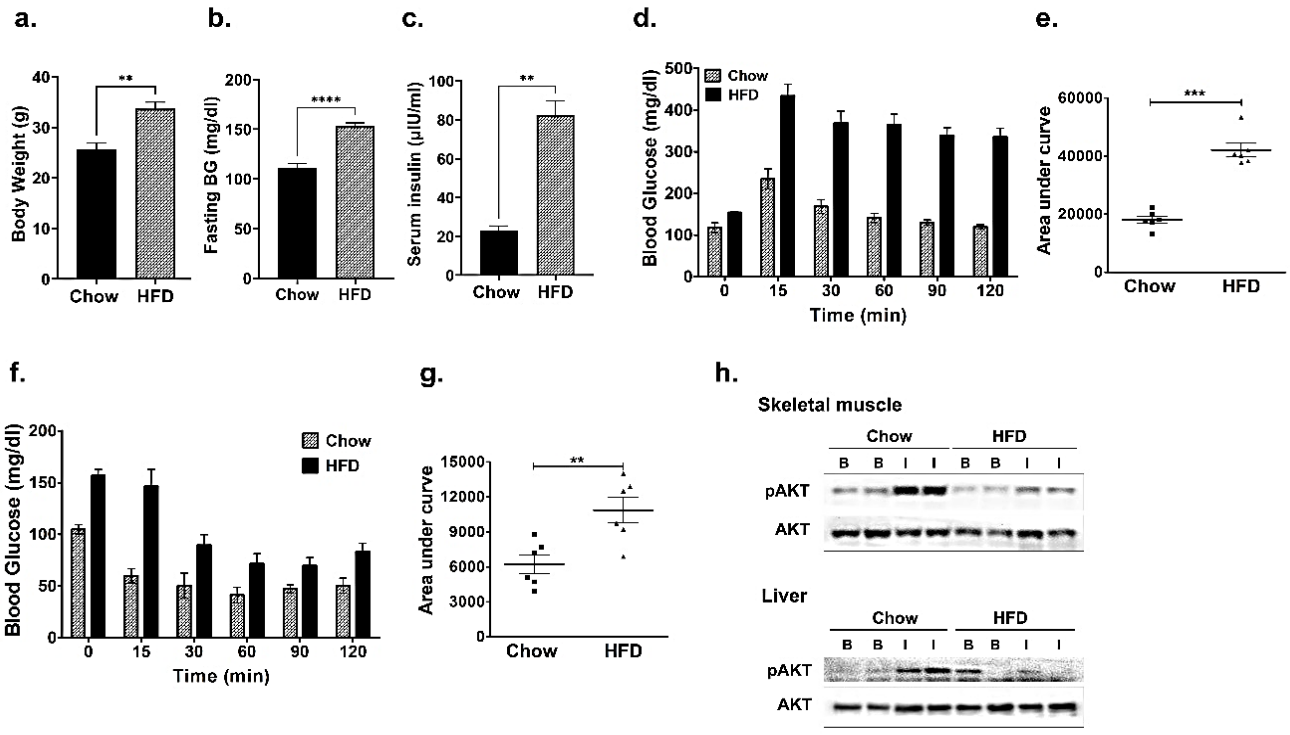

Figure 1: Validation of HFD-induced mice model of IR. The male C57BL/6J mice were kept on CD or HFD for 16 weeks. Shown are the effect on body weight **(a)**, fasting blood glucose level **(b)**, serum insulin level **(c),** glucose tolerance **(d** and **e),** insulin tolerance **(f** and **g)** and insulin-stimulated Akt (Ser-473) phosphorylation in skeletal muscle and liver **(h)** after 16 weeks. B; basal, I; insulin treated group. Data are mean±SE, n=6, **p<0.01 and ****p<0.001.

2. **Metabolic Changes in IR Mice:** We performed univariate analysis on 75 annotated metabolites identified through GC-MS/MS-based untargeted metabolomics approach in HFD-fed mice serum samples (Supplementary Data 1). Fold change analysis with threshold value of 2.0 identified that total 27 metabolites were characterized by increased concentration and 31 metabolites were down-accumulated in HFD-fed mice, whereas 16 metabolites were not significantly altered (Supplementary Data 1). The t-test analysis pointed out that 22 metabolites out of 75 (p-value ≤ 0.05) were significantly altered in insulin-resistant mice fed with HFD. The T-stat value highlights that 6 out of 22 have a lower concentration (positive t-stat value) and 16 out of 22 were increasing in concentration (negative t-stat value) in HFD-fed insulin-resistant mice **(Table 1)**.

Table 1. Outcomes of T-test analysis of metabolites data comparing individual metabolites in CD mice samples with HFD mice samples (p-value <0.05).

Metabolites Name	t.stat	p.value	-log10(p)
Stearic acid	-9.095	9.92E-05	4.0034
L-Malic acid	8.7058	0.000127	3.8965
Cholesterol	-6.8769	0.000466	3.3314
Mannitol	5.7725	0.00118	2.928
L-Lysine	-5.1162	0.002187	2.6603
Xylitol	4.9102	0.002683	2.5714
S-Carboxymethyl-L-cysteine	-4.9074	0.002691	2.5701
abietic acid	-4.7739	0.003082	2.5111
Linoleic acid	-4.4576	0.004294	2.3671
Diethanolamine	-4.1177	0.006232	2.2054
Phenylalanine	4.1014	0.006347	2.1974
isohexonic acid	3.6755	0.010386	1.9835
Melibiose	-3.4419	0.013769	1.8611
beta-sitosterol	-3.4387	0.013823	1.8594
D-Glucose 6-phosphate	-3.2561	0.017333	1.7611
Tryptamine	-3.1026	0.021047	1.6768
Noradrenaline	-2.9785	0.024683	1.6076
Uridine 5'-diphospho-N-acetylglucosamine	-2.8478	0.029268	1.5336
Threonic acid	2.8228	0.030243	1.5194
2_3-Diaminopropionic acid	-2.6643	0.037311	1.4282
Glycerol 3-phosphoate	-2.5338	0.044451	1.3521
D-Penicillamine	-2.4601	0.04911	1.3088

Further, we performed volcano plot analysis, combining fold change and P-value (FC > 2.0, p-value ≤ 0.05). The results of the volcano plot analysis showed that 16 metabolites were

significantly up-accumulated, whereas 6 were down-accumulated in mice serum samples after 16 weeks of HFD feeding **(Fig. 2) (Table 2)**.

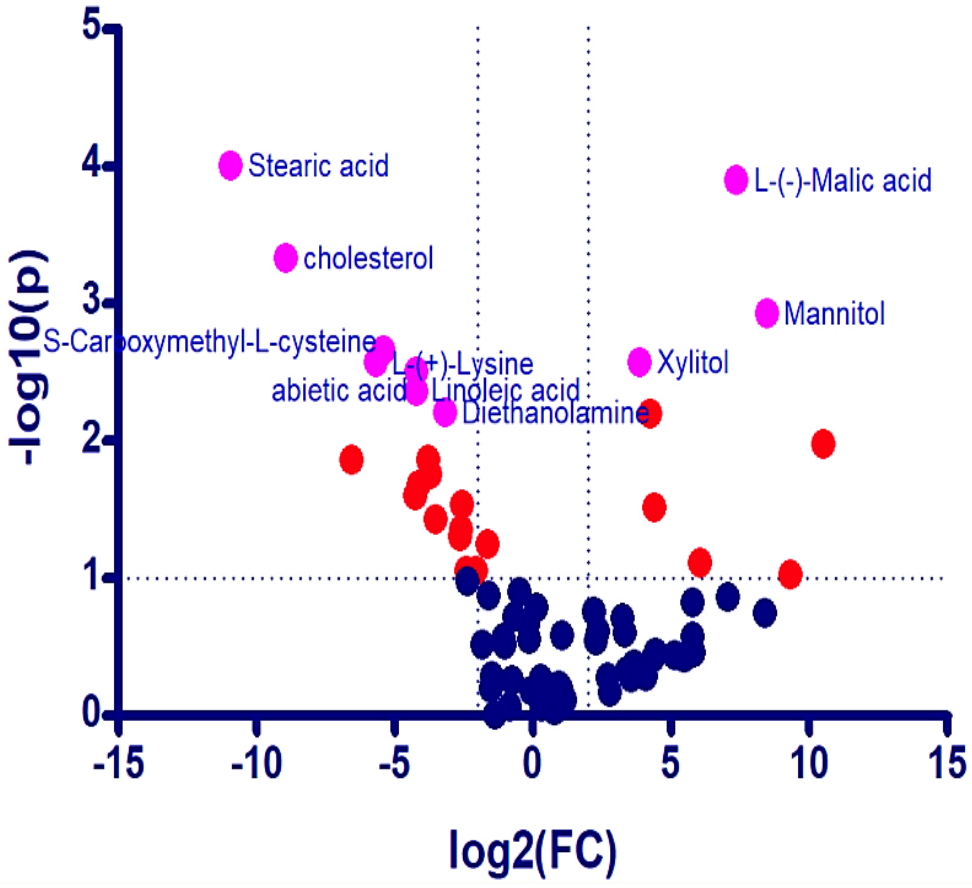

Figure 2: Volcano plot representing differential metabolites in insulin-resistant mice fed with CD. Fold Change >2.0, P-value ≤ 0.05 (in red) shows significantly altered metabolites between CD and HFD mice. Fold Change >2.0, P-value ≤ 0.05 (in pink) highlights the top 10 significant metabolites between the two groups.

Table 2. Metabolites that have more than 2-fold high and low accumulation after 16 weeks of HFD-fed mice compared to CD-fed mice (p-value <0.05, FC >2.0).

Metabolites Name	**FC**	**log2(FC)**	**p-value**	**-log10(p)**
Stearic acid	0.00051	-10.938	9.92E-05	4.0034
L-Malic acid	161.8	7.3381	0.000127	3.8965
Cholesterol	0.002035	-8.9407	0.000466	3.3314
Mannitol	346.49	8.4367	0.00118	2.928
L-Lysine	0.023519	-5.41	0.002187	2.6603
Xylitol	14.388	3.8467	0.002683	2.5714

S-Carboxymethyl-L-cysteine	0.019154	-5.7062	0.002691	2.5701
abietic acid	0.0533	-4.2297	0.003082	2.5111
Linoleic acid	0.05374	-4.2179	0.004294	2.3671
Diethanolamine	0.10856	-3.2034	0.006232	2.2054
Phenylalanine	18.88	4.2388	0.006347	2.1974
isohexonic acid	1416.3	10.468	0.010386	1.9835
Melibiose	0.010569	-6.564	0.013769	1.8611
beta-sitosterol	0.071252	-3.8109	0.013823	1.8594
D-Glucose 6-phosphate	0.075062	-3.7358	0.017333	1.7611
Tryptamine	0.055695	-4.1663	0.021047	1.6768
Noradrenaline	0.051604	-4.2764	0.024683	1.6076
Uridine 5'-diphospho-N-acetylglucosamine	0.1654	-2.5959	0.029268	1.5336
Threonic acid	20.575	4.3628	0.030243	1.5194
2_3-Diaminopropionic acid	0.085848	-3.5421	0.037311	1.4282
Glycerol 3-phosphoate	0.1612	-2.6331	0.044451	1.3521
D-Penicillamine	0.15981	-2.6456	0.04911	1.3088

The heat map, contained 22 distinct metabolites in the two groups and provided a global picture of metabolic aspects. Remarkably, higher level of fatty acids or lipid-like molecules, such as palmitic acid, linoleic acid, stearic acid, cholesterol and beta-sitosterol were found; however, serum level of different amino acids was significantly decreased in insulin-resistant mice after intake of HFD for 16 weeks **(Fig. 3)**.

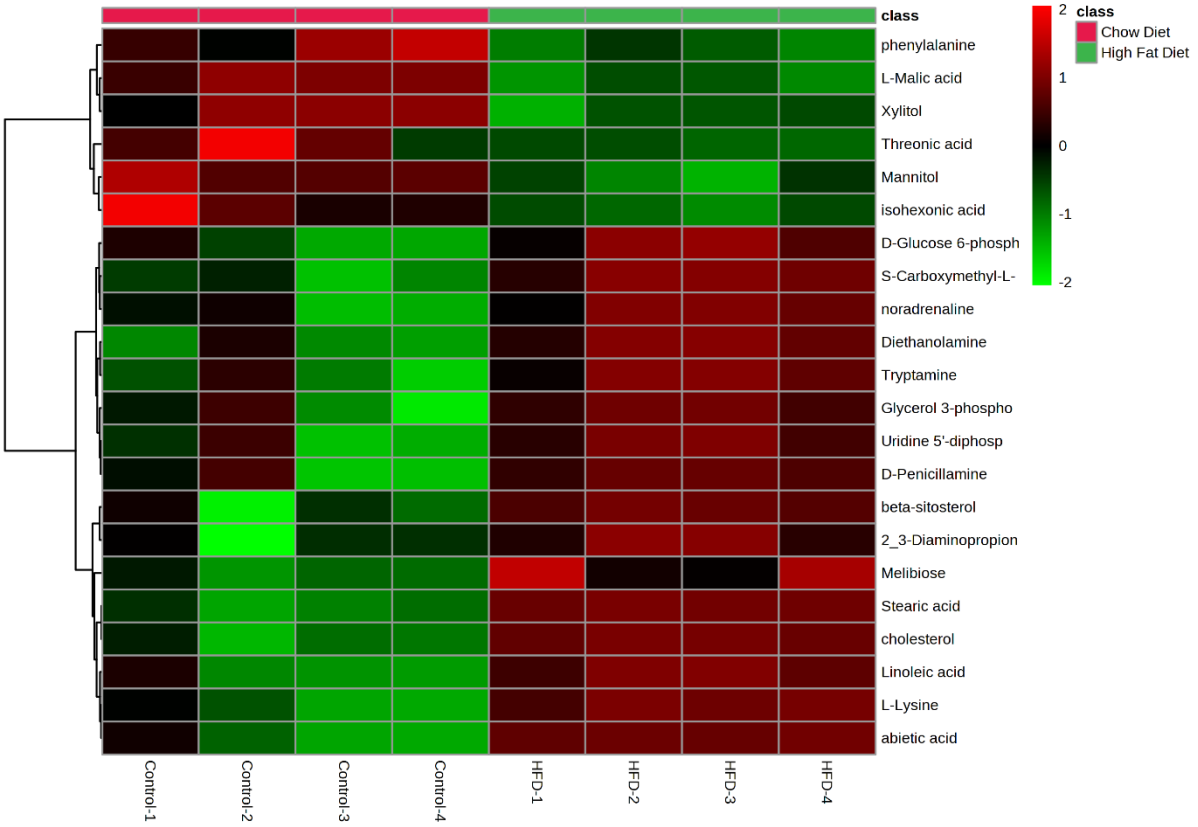

Figure 3: Heat Map of GC-MS/MS based top 22 differential metabolites between mice fed with CD and HFD (distance measure using Euclidean, and clustering algorithm using ward). Change in colours from green to red represents the higher concentration of metabolites in particular samples. (Control 1-4 = Mice fed with CD, HFD 1-4 = Mice fed with HFD).

3. Multivariate Analysis: To evaluate the robustness of the GC-MS/MS based serum metabolomics profiling, multivariate analysis such as principal component analysis (PCA) and orthogonal partial least square discriminant analysis (OPLS-DA) were performed. The multivariate analysis assessed metabolites in groups and individuals, allowing for sample differentiation. Among all the analyzed samples, 75 annotated metabolites were allowed for metabolomics data analysis and retrieval of 2419 unknown EI-MS common characteristics (Supplementary Data 1).

PCA score plots of the first two components obtained from GC-MS/MS pointed out a clear separation between the insulin-resistant mice fed with an HFD (n=4, green circle) from the group fed with CD (n=4, red circle). The first principal component (PC1) explains 46.2% of

the total variability, whereas PC2 has 22.9% **(Fig. 4a)**. The loadings plot highlighted that the PC1 was mainly dominated by inositol, stearic acid, galactitol, D-penicillamine, and D-galactose, whereas the PC2 by D-mannose, tyrosine, creatinine, isocitric acid, 2,3-diaminopropionic acid, hexose, cholesterol, stearic acid, heptadecanic acid and sorbitol **(Fig. 4b)**.

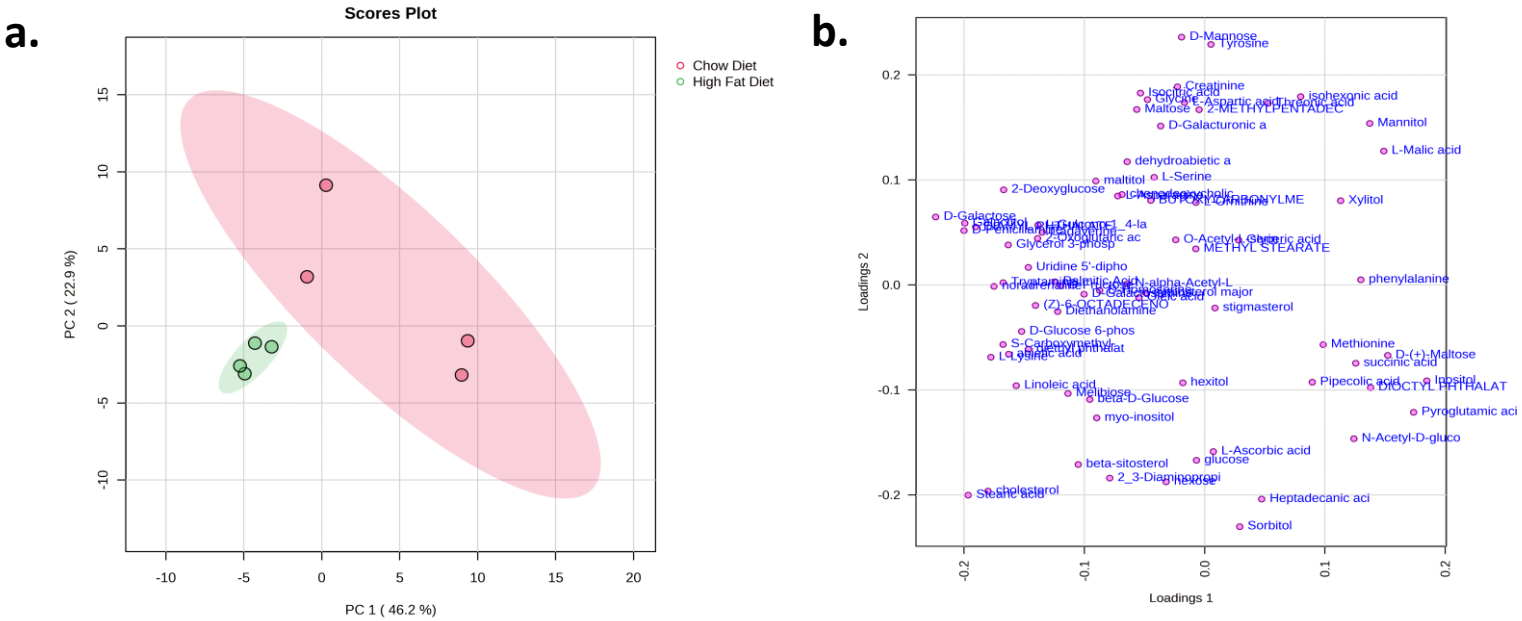

Figure 4: Multivariate statistical analysis based on un-targeted GC-MS/MS based metabolomic profiling data from serum samples of insulin resistant mice fed with CD (n=4, red circle) and HFD (n=4, green circle). a) PCA score plots of the first two components obtained from GC-MS/MS represent complete metabolite class isolation between two study groups. b) PCA loadings plot of PC2 versus PC1 from quantified serum metabolites of HFD and CD mice.

The compact clustering of the HFD replicates (green circles) represents the high reproducibility of the GC-MS/MS analysis. Groups separation was further confirmed by the OPLS-DA analysis with 95% confidence interval, where the T-score was 33.7%, and the Orthogonal T score was 30.7% **(Fig. 5a)**. As per the OPLS-DA derived loading (VIP scores), 15 metabolites were identified that contributed significantly to groups separation (Supplementary Data 1). Six of them (Malic acid, xylitol, mannitol, isohexanoic acid, phenylalanine and Threonic acid) were significantly down-accumulated. In contrast, the

remaining 9 (Cholesterol, linolenic acid, stearic acid, abietic acid, lysine, diethanolamine, beta-sitosterol, S-Carboxymethyl-L-cysteine and Glucose 6-phosphate) were characterized by increased concentration in serum of HFD-fed mice (**Fig. 5b and Supplementary Data 1**). The study model was validated through permutation and cross-validation to avoid overfitting. The permutation test supported our study model's robustness and our data's reproducibility (p-value $\leq$ 0.05), and cross-validated coefficient R2Y (0.988) and Q2 (0.762) shows the goodness of fit **(Fig. 5c and d)**.

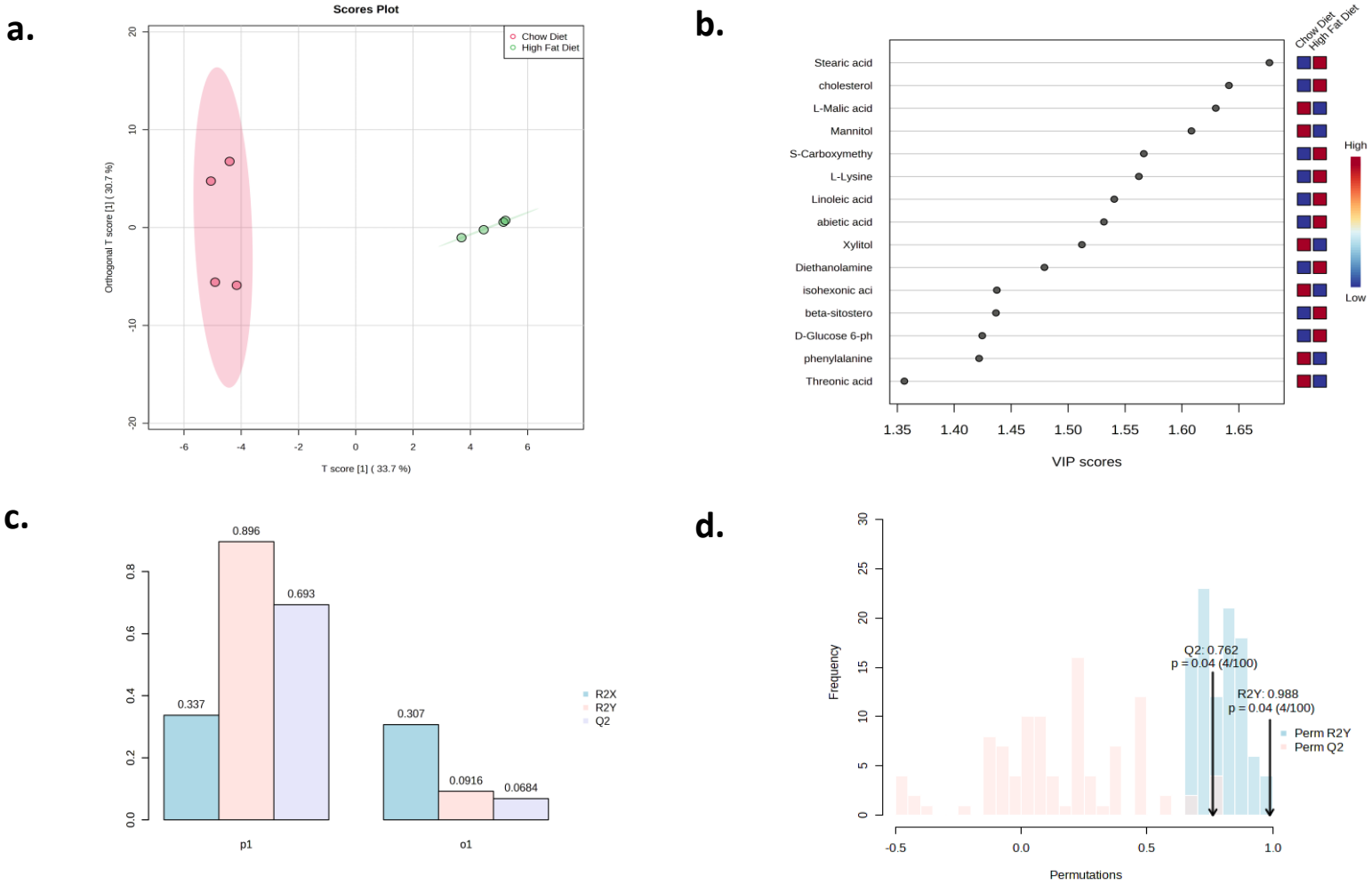

Figure 5: OPLS-DA analysis. a) The OPLS-DA model represents the CD mice (red circle) and HFD (blue circle), confirming the separation between the two groups, where the T-score was 33.7%, and Orthogonal T score was 30.7%. The shaded ellipses around each group (n=4) represent 95% confidence interval estimated from the score; b) VIP scores showing the top 15 metabolites identified through GC-MS/MS analysis and most important for two study groups discrimination. c) Model overview of the OPLS-DA model for the provided dataset. It

shows the R2X, R2Y, and Q2 coefficients for the groups; d) 2000-times permutation analysis of the model indicates the stability of our study model.

4. Alteration in metabolic pathways in insulin resistant mice: To detect physiologically relevant patterns, data concerning 16 weeks of HFD in insulin resistant mice were further analyzed through the metaboanalyst tool in KEGG-based pathway analysis. The comparative metabolomic profiling of HFD-fed insulin-resistant mice with CD-fed mice, identified 4 significantly affected metabolic pathways with impact score > 0.05 and p-value ≤ 0.05 **(Fig. 6)**.

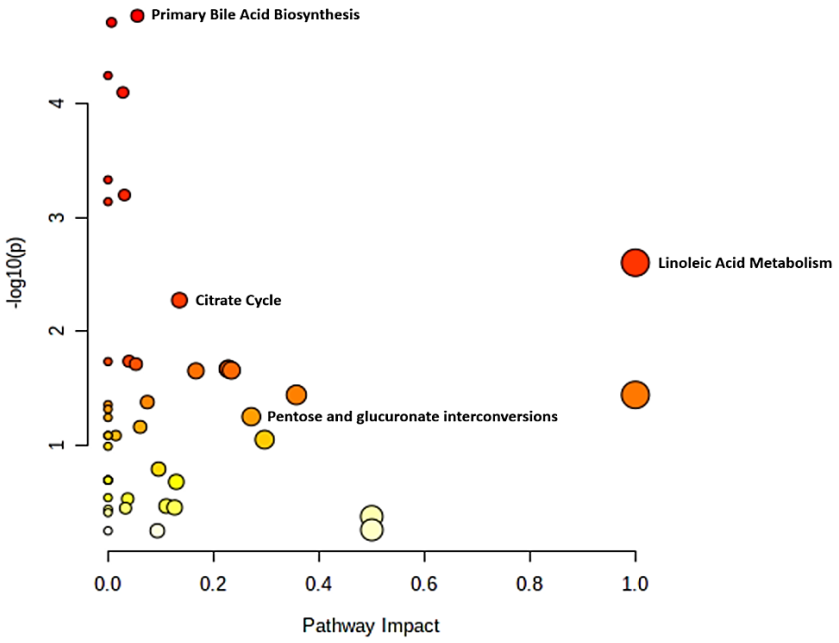

Pathway Name	Total Cmpd	Hits	Raw p	-log10 (p)	Holm adjust	FDR	Impact	Upregulated
Primary bile acid biosynthesis	46	3	1.72E-05	4.7645	0.000791	0.000452	0.05563	HFD
Linoleic acid metabolism	5	1	0.0024952	2.6029	0.097314	0.014348	1	HFD
Pentose and glucuronate interconversions	18	1	0.003951	2.4033	0.15014	0.020194	0.17188	CD
Citrate cycle (TCA cycle)	20	3	0.0053125	2.2747	0.19656	0.024437	0.13541	CD

Figure 6: Pathway analysis from Metaboanalyst 5.0. The top enriched and impacted metabolic pathway of physiological importance in insulin-resistant mice. The X-axis represents pathway impact, whereas Y-axis represent -$\log_{10}$ (p) value. The size of the circles

represents the enrichment of the pathway, and the intensity of the red colour represents a higher statistical significance.

In significantly altered metabolic pathways, primary bile acid biosynthesis and linoleic acid metabolism were upregulated in HFD group; whereas pentose and glucuronate interconversions, and citrate cycle (TCA cycle) were downregulated in mice fed with HFD **(Fig. 7)**.

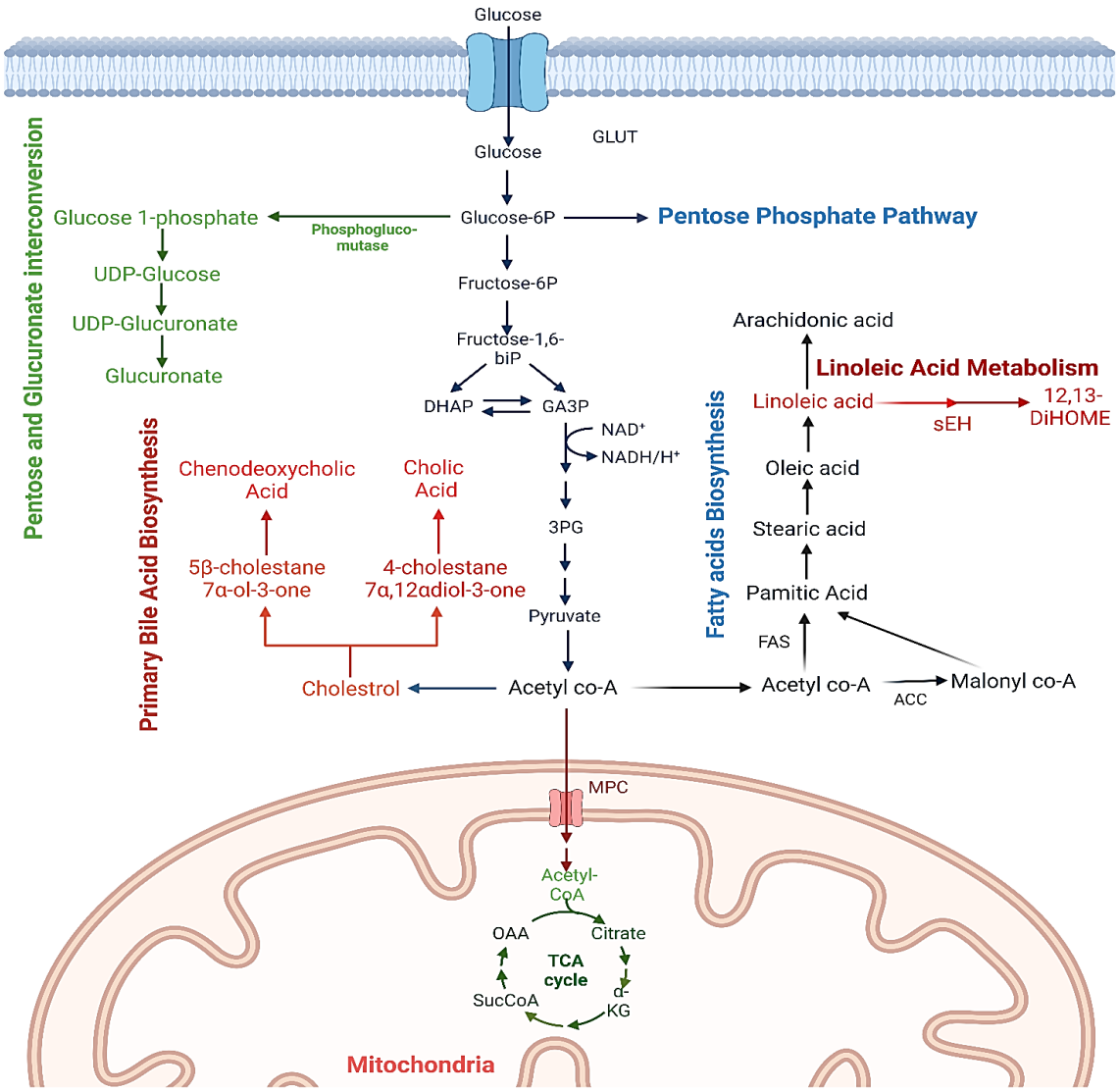

Figure 7: Schematic representation of altered metabolic pathways in insulin resistant mice fed with HFD for 16 weeks. Red colour depicts Pathway upregulated whereas green colour is representative of pathways downregulated in HFD-fed insulin resistant mice.

5. Identification of metabolomics-based IR Biomarkers: Biomarker analyses were carried out to identify the least number of metabolites needed to illustrate and interpret the difference between IR mice fed with HFD and control CD-fed mice. In this study, the support vector machine (SVM) with 3 metabolites has good AUROC (0.86, 95% CI= 0-1), and increasing the number of metabolites up to 5 increased AUROC (0.96, 95% CI= 0.225-1) near perfect. Further increasing the number from 10 metabolites to 74 AUROC reached perfect values (1, 95% CI=1-1) **(Fig. 8a)**. Similar results were observed on predictive accuracies with number of different features where the addition of 34 metabolites increased accuracy by 9%. While reaching a number of 74 features, predictive accuracy increased by only 2% **(Fig. 8b)**.

The variables chosen in the SVM model with 37 metabolites. All the 22 metabolites that were statistically significant in t-test were significantly altered in the serum of mice fed with HFD or CD in biomarker analysis (p-value ≤ 0.05). Interestingly; some of the statistically non-significant (p-value > 0.05) metabolites were also selected namely, galactose, galactitol, palmitic acid, 2 oxoglutaric acid, hexose, hexitol, homoserine, maltose, methyl pentadecanoic acid, N-alpha-acetyl-L-ornithine, creatinine, O-acetyl-L-serine, L-serine and L-aspartic acid but these metabolites were significantly altered in log 2-fold change analysis **(Fig. 8c)**.

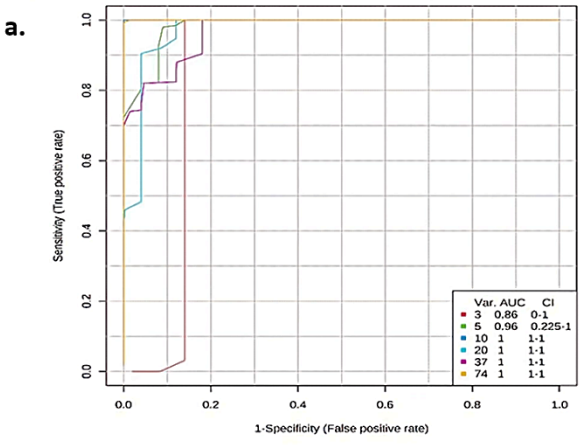

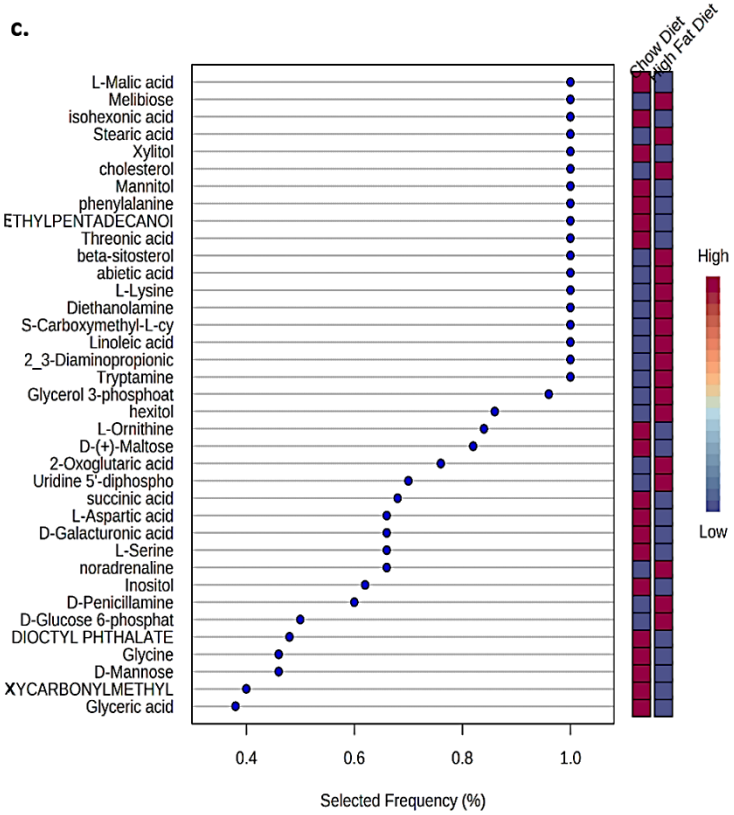

Figure 8: Metabolomic based biomarker analysis. a) Model performance test for all 6-support vector machine (SVM) classifier with continuously enhancing the number of metabolites. ROC curve of each SVM classifier based on average cross-validation performance. AUC and CI of 95% are displayed in the panel. b) predictive accuracy with different features for 6 different SVM. The model shows the highest accuracy with 74 metabolites highlighted in red. c) Important 37 variables for classification of HFD mice to CD mice from the SVM model.

Discussion:

The IR is a characteristic feature of metabolic syndrome and a precursor to development of T2DM and associated metabolic complications. However, the contributory and causative factors leading to IR remained largely uncertain. Although, IR has been known to be associated with obesity and excess accumulation of triglycerides, the exact relationship of obesity with IR is obscure. The diagnosis of diabetes is an end point that represent itself very late when many organ systems are already affected. Thus, there is a need to understand the early abnormalities that are associated during the development of IR, leading to T2DM.

Increased consumption of HFD and physical idleness lead to obesity which a leading factor in the pathogenesis of metabolic syndrome.[27] There is a profound significance of metabolic alterations and perturbations in obese subjects making them susceptible to IR. Advanced LC/MS techniques were used for identification of lipid biomarkers, characterization of other metabolites are still explored.[28-29] Obese mice induced by HFD exhibit marked metabolic differences.[12] The selected and targeted metabolites of glycolysis, the tricarboxylic acid (TCA) cycle, glutaminolysis, and fatty acid β-oxidation in HFD-fed obese mice have been profiled by using gas chromatography earlier.[13] This study included 8 week old HFD mice. We performed the untargeted metabolic profiling in the obese mice fed with HFD for 16 weeks. The longer span of HFD allowed the establishment of IR phenotype (Fig.1). To best of our knowledge, for the first time, untargeted full scan metabolite analysis of insulin resistant mice allowed us to look into a diverse array of metabolic pathways as well as look into potential biomarkers. This information may potentially enable us to characterize

metabolic transformations that take place during the progression of IR to T2DM. A study conducted on 4-16 weeks HFD-fed mice characterized the role of metabolites at different time points in Inducing Non-alcoholic Fatty Liver Disease.[14] Analysis of the metabolomic profile revealed marked differences in metabolites between the control and HFD group depending upon NAFLD severity resulting in shortlisting of a total of 30 potential biomarkers strongly associated with the development of NAFLD.

In the present study, a rodent model of HFD-fed mice was used for untargeted metabolomic profiling using GC-MS/MS. Mice fed on HFD for 16 weeks displayed metabolic alterations characterized by glucose and insulin intolerance and impaired insulin-stimulated phosphorylation of Akt (Ser-473), a key node of insulin signalling cascade; validating the induction of IR in HFD-fed mice.[26] Therefore, the metabolic profiling of HFD-induced IR mice may provide important information to increase our understanding of the pathophysiology of IR and metabolic syndrome. Serum Metabolic profiling identified higher accumulation of lipid and steroid such as cholesterol, linoleic acid, stearic acid and beta-sitosterol in HFD-induced insulin reisitant mice. In contrast, CD mice have higher accumulation of sugar acids e.g., malic acid, Threonic acid, hexanoic acid etc.

Our findings revealed that HFD-induced metabolic changes resulted in the modulation of key metabolic pathways involved in bile acid synthesis, linoleic acid metabolism, pentose and gluconate inter conversions and TCA cycles. Bile acids are crucial physiological agents, in addition to their role in nutrient absorption they also act as signalling molecule to regulate nutrient metabolism and to establish metabolic homeostasis.[30] Our metabolomics profiling indicated upregulation of bile acid synthesis pathway in HFD-fed IR mice. We also observed increased cholesterol level in HFD-fed mice. Therefore, activation of bile acid metabolism in our study reflects the expected physiological changes where increase in cholesterol and bile acids are required for efficient digestion and absorption of HFD ingredients. Cholesterol is

the precursor for the synthesis of bile acid which intern involved in multiple activities including absorption of fat- and fat-soluble vitamins.[31] In support, involvement of raised bile acid metabolism in glucose homeostasis, a cross-sectional study revealed that IR in males had associated with hyper bile acidaemia in both diabetic and non-diabetic participants and associated positively to IR.[32] Another metabolomic study during oral glucose tolerance showed decreased level of fatty acids and rise of bile acids in biphasic manner.[33] These studies along with our data support the implication of bile acid metabolism in pathogenesis of IR.

In HFD-fed mice model, fatty acids become the primary source of energy over glucose. Therefore, IR generally associated with increased fatty acid oxidation and an overall decrease in glycolysis and utilization of glucose.[34] Excessive dependence on fatty acid oxidation as an energy source can increase oxygen cost leading to increased ROS, further contributing to induction/ progression of IR.[35] In our study, development of HFD-induced IR was associated with increased concentration of free fatty acids including, linolenic acid, stearic acid and palmitic acid, suggesting the pathogenic role of fatty acids in the development of IR. Importantly, we observed up regulated linoleic acid metabolism in HFD-fed mice and it could to a protective mechanism to metabolize higher level of fatty acid in HFD-fed condition. Importantly, conjugated linoleic acid supplementation adversely affect insulin and glucose metabolism in T2DM patient.[36] The study supports our metabolomics data and provide linoleic acid as an indicator of IR development.

The tricarboxylic acid (TCA) cycle leads to final oxidation of fat and is the main source of electron for respiration and metabolic progenitor of gluconeogenesis. The HFD-induced impairment in TCA cycle has been demonstrated to cause dysfunctional mitochondrial activity, contributing to development of IR. The process enables feeding of electrons into an inefficient respiratory chain making the physiology susceptible to increase ROS and by

providing mitochondria derived substrate for gluconeogenesis, further contribute to mitochondrial dysfunction.[37] We also observed impairment of TCA cycle in mice fed on HFD for 16 weeks in our metabolomics profiling, verifying its role as a biomarker and therapeutic target for IR. Another pathway revealed by analysis for top enriched and impacted metabolic mechanism was galactose metabolism. Higher galactose levels have been correlated with IR in patients with polycystic ovary syndrome.[38] In D-galactose induced aging model, higher concentration of galactose leads to cardiac dysfunction.[39] In the present study also the galactose metabolic pathways were positively associated with IR in HFD-induced mice model, validating the role of galactose metabolism in IR development.

Diet-induced obesity is the leading cause of the of patients diagnosed with metabolic disorders such as T2DM, cardiovascular disease or atherosclerosis.[40] Ceramides are important bioactive lipids capable of regulating activity of enzymes as well as transcription factors.[41-43] Human studies indicate a connection between ceramides and IR. Elevated ceramides are reported in individuals with obesity in association with muscle IR.[44-45] Correlations between liver ceramides content and hepatic IR in fatty liver disease are also known.[46] GC analysis in the mice samples did not detect Ceramide class of metabolites; a limitation in the present study.

Analysis of metabolome of patients with obesity or T2DM compared with healthy control revealed that BCAA and glutamine metabolism and urea cycle constitute major metabolomic changes.[47] In fact usage of Metabolomics in obesity has been examined widely. Untargeted metabolomic profiling was performed on fasting serum samples from 27 obese and adolescents and 15 sex- and age-matched healthy children. Three metabolomic assays were combined and yielded 726 unique identified metabolites by using GC–MS) and liquid chromatography-mass spectrometry (LC–MS). Children with obesity had higher concentrations of branch-chained amino acids and various lipid metabolites, including

phosphatidylcholines, cholesteryl esters, triglycerides.[48] Both these studies indicated involvement of altered BCAA and lipid metabolism, similar to the data presented in our study. Non-pharmological interventions such as exercise training can benefit obese subjects via altering their metabolomc profiles leading to reduced IR.[49]

In summary, the serum samples from the HFD-fed IR and CD-fed mice were compared and characterized using metabolomic profile to provide new instincts related to development of IR. Substantial alterations were reported in metabolic pathways leading to bile acid biosynthesis, fatty acid metabolism, pentose-glucuronate interconversion and TCA cycle. The metabolites of the primary bile acid biosynthesis and linoleic acid metabolism were upregulated and positively correlated with IR; whereas metabolites of Pentose and glucuronate interconversions, and TCA cycle were significantly decreased and negatively associated with development of HFD-induced IR. Results of biomarker analysis identified metabolites that are potentially involved in the altered metabolic pathways. Hence, key metabolite of these altered pathways could be exploited as biomarker for diet- induced IR. Our study also revealed the use of GC-MS/MS based untargeted metabolomic profiling as an effective analytical tool to illustrate metabolomic profile in diet-induced IR.

Funding: Manendra Singh Tomar is the recipient of Junior research fellowship from the University Grants Commission, Government of India. Aditya Sharma is recipient of research fellowship from the Council of Scientific and Industrial Research (CSIR), Govt. of India. Ankit Pateriya is recipient of research fellowship from the Indian Council of Medical Research (ICMR), Govt. of India. Extramural research grant (No. BT/PR15667/BRB/10/1465/2015) from the Department of Biotechnology, New Delhi, India to Akhilesh Kumar Tamrakar is highly acknowledged. Laboratory of Ashutosh Shrivastava is supported by CCRH-Ministry of AYUSH, Government of India.

Author's contributions: **AKT** and **AS** conceptualized and planned the manuscript. **MST ADS** and **AP** performed the experiment. **MST**, **FA**, **AKT** and **AS** analysed and interpreted the data of the study. **MST**, **AKT** and **AS** wrote the manuscript. All authors concur to the final version of the manuscript.

Declaration of interest: Authors declare no conflict of interest.

Associated content: Supplementary File S1 containing raw and analyzed data sets.

Abbreviations:

CD; Chow Diet

GC-MS/MS; Gas Chromatography tandem Mass Spectrometry

HFD; High Fat Diet

IR; Insulin Resistance

OPLS-DS; Orthogonal partial Least Square-Discriminant Analysis

PCA; Principal Component Analysis

ROC: Receiver Operating Curve

SVM; Support Vector Machine

SDS-PAGE; Sodium dodecyl-sulfate polyacrylamide gel electrophoresis

T2DM; Type II Diabetes Mellitus

References:

1. Yuan, H. X.; Xiong, Y.; Guan, K. L., Nutrient sensing, metabolism, and cell growth control. *Molecular cell* **2013,** *49* (3), 379-87. 10.1016/j.molcel.2013.01.019.
2. Haeusler, R. A.; McGraw, T. E.; Accili, D., Biochemical and cellular properties of insulin receptor signalling. *Nature reviews. Molecular cell biology* **2018,** *19* (1), 31-44. 10.1038/nrm.2017.89.
3. Czech, M. P., Insulin action and resistance in obesity and type 2 diabetes. *Nature medicine* **2017,** *23* (7), 804-814. 10.1038/nm.4350.
4. Eckel, R. H.; Grundy, S. M.; Zimmet, P. Z., The metabolic syndrome. *Lancet (London, England)* **2005,** *365* (9468), 1415-28. 10.1016/S0140-6736(05)66378-7.
5. Galicia-Garcia, U.; Benito-Vicente, A.; Jebari, S.; Larrea-Sebal, A.; Siddiqi, H.; Uribe, K. B.; Ostolaza, H.; Martín, C., Pathophysiology of Type 2 Diabetes Mellitus. *International journal of molecular sciences* **2020,** *21* (17). 10.3390/ijms21176275.
6. Black, M. H.; Watanabe, R. M.; Trigo, E.; Takayanagi, M.; Lawrence, J. M.; Buchanan, T. A.; Xiang, A. H., High-fat diet is associated with obesity-mediated insulin resistance and β-cell dysfunction in Mexican Americans. *The Journal of nutrition* **2013,** *143* (4), 479-85. 10.3945/jn.112.170449.
7. Fruh, S. M., Obesity: Risk factors, complications, and strategies for sustainable long-term weight management. *Journal of the American Association of Nurse Practitioners* **2017,** *29* (S1), S3-s14. 10.1002/2327-6924.12510.
8. Nguyen, D. M.; El-Serag, H. B., The epidemiology of obesity. *Gastroenterology clinics of North America* **2010,** *39* (1), 1-7. 10.1016/j.gtc.2009.12.014.
9. Gan, W. Z.; Ramachandran, V.; Lim, C. S. Y.; Koh, R. Y., Omics-based biomarkers in the diagnosis of diabetes. *Journal of Basic and Clinical Physiology and Pharmacology* **2020,** *31* (2). 10.1515/jbcpp-2019-0120.
10. Hameed, A.; Mojsak, P.; Buczynska, A.; Suleria, H. A. R.; Kretowski, A.; Ciborowski, M., Altered Metabolome of Lipids and Amino Acids Species: A Source of Early Signature Biomarkers of T2DM. *Journal of clinical medicine* **2020,** *9* (7). 10.3390/jcm9072257.
11. Bain, J. R.; Stevens, R. D.; Wenner, B. R.; Ilkayeva, O.; Muoio, D. M.; Newgard, C. B., Metabolomics applied to diabetes research: moving from information to knowledge. *Diabetes* **2009,** *58* (11), 2429-43. 10.2337/db09-0580.
12. Bao, L.; Yang, C.; Shi, Z.; Wang, Z.; Jiang, D., Analysis of Serum Metabolomics in Obese Mice Induced by High-Fat Diet. *Diabetes, metabolic syndrome and obesity : targets and therapy* **2021,** *14*, 4671-4678. 10.2147/DMSO.S337979.
13. Patel, D. P.; Krausz, K. W.; Xie, C.; Beyoğlu, D.; Gonzalez, F. J.; Idle, J. R., Metabolic profiling by gas chromatography-mass spectrometry of energy metabolism in high-fat diet-fed obese mice. *PloS one* **2017,** *12* (5), e0177953. 10.1371/journal.pone.0177953.
14. Lai, Y. S.; Chen, W. C.; Kuo, T. C.; Ho, C. T.; Kuo, C. H.; Tseng, Y. J.; Lu, K. H.; Lin, S. H.; Panyod, S.; Sheen, L. Y., Mass-Spectrometry-Based Serum Metabolomics of a C57BL/6J Mouse Model of High-Fat-Diet-Induced Non-alcoholic Fatty Liver Disease Development. *Journal of agricultural and food chemistry* **2015,** *63* (35), 7873-84. 10.1021/acs.jafc.5b02830.
15. Boden, G.; Shulman, G. I., Free fatty acids in obesity and type 2 diabetes: defining their role in the development of insulin resistance and beta-cell dysfunction. *European journal of clinical investigation* **2002,** *32 Suppl 3*, 14-23. 10.1046/j.1365-2362.32.s3.3.x.
16. Xu, X.; Grijalva, A.; Skowronski, A.; van Eijk, M.; Serlie, M. J.; Ferrante, A. W., Jr., Obesity activates a program of lysosomal-dependent lipid metabolism in adipose tissue

macrophages independently of classic activation. *Cell metabolism* **2013,** *18* (6), 816-30. 10.1016/j.cmet.2013.11.001.
17. Burla, B.; Arita, M.; Arita, M.; Bendt, A. K.; Cazenave-Gassiot, A.; Dennis, E. A.; Ekroos, K.; Han, X.; Ikeda, K.; Liebisch, G.; Lin, M. K.; Loh, T. P.; Meikle, P. J.; Orešič, M.; Quehenberger, O.; Shevchenko, A.; Torta, F.; Wakelam, M. J. O.; Wheelock, C. E.; Wenk, M. R., MS-based lipidomics of human blood plasma: a community-initiated position paper to develop accepted guidelines. *Journal of lipid research* **2018,** *59* (10), 2001-2017. 10.1194/jlr.S087163.
18. Yang, Q.; Vijayakumar, A.; Kahn, B. B., Metabolites as regulators of insulin sensitivity and metabolism. *Nature reviews. Molecular cell biology* **2018,** *19* (10), 654-672. 10.1038/s41580-018-0044-8.
19. Yue, J. T.; Lam, T. K., Lipid sensing and insulin resistance in the brain. *Cell metabolism* **2012,** *15* (5), 646-55. 10.1016/j.cmet.2012.01.013.
20. Youn, J. H., Fat sensing and metabolic syndrome. *Reviews in endocrine & metabolic disorders* **2014,** *15* (4), 263-75. 10.1007/s11154-014-9300-1.
21. Sharma, A.; Singh, S.; Mishra, A.; Rai, A. K.; Ahmad, I.; Ahmad, S.; Gulzar, F.; Schertzer, J. D.; Shrivastava, A.; Tamrakar, A. K., Insulin resistance corresponds with a progressive increase in NOD1 in high fat diet-fed mice. *Endocrine* **2022,** *76* (2), 282-293. 10.1007/s12020-022-02995-z.
22. Mohit; Tomar, M. S.; Araniti, F.; Pateriya, A.; Singh Kushwaha, R. A.; Singh, B. P.; Jurel, S. K.; Singh, R. D.; Shrivastava, A.; Chand, P., Identification of metabolic fingerprints in severe obstructive sleep apnea using gas chromatography–Mass spectrometry. *Frontiers in Molecular Biosciences* **2022,** *9*. 10.3389/fmolb.2022.1026848.
23. Tsugawa, H.; Cajka, T.; Kind, T.; Ma, Y.; Higgins, B.; Ikeda, K.; Kanazawa, M.; VanderGheynst, J.; Fiehn, O.; Arita, M., MS-DIAL: data-independent MS/MS deconvolution for comprehensive metabolome analysis. *Nature methods* **2015,** *12* (6), 523-6. 10.1038/nmeth.3393.
24. Sansone, S. A.; Fan, T.; Goodacre, R.; Griffin, J. L.; Hardy, N. W.; Kaddurah-Daouk, R.; Kristal, B. S.; Lindon, J.; Mendes, P.; Morrison, N.; Nikolau, B.; Robertson, D.; Sumner, L. W.; Taylor, C.; van der Werf, M.; van Ommen, B.; Fiehn, O., The metabolomics standards initiative. *Nature biotechnology* **2007,** *25* (8), 846-8. 10.1038/nbt0807-846b.
25. Kong, Q.; Gu, J.; Lu, R.; Huang, C.; Hu, X.; Wu, W.; Lin, D., NMR-Based Metabolomic Analysis of Sera in Mouse Models of CVB3-Induced Viral Myocarditis and Dilated Cardiomyopathy. *Biomolecules* **2022,** *12* (1). 10.3390/biom12010112.
26. Taniguchi, C. M.; Emanuelli, B.; Kahn, C. R., Critical nodes in signalling pathways: insights into insulin action. *Nature reviews. Molecular cell biology* **2006,** *7* (2), 85-96. 10.1038/nrm1837.
27. Després, J. P.; Lemieux, I., Abdominal obesity and metabolic syndrome. *Nature* **2006,** *444* (7121), 881-7. 10.1038/nature05488.
28. Ando, A.; Satomi, Y., A Simple and Highly Sensitive Quantitation of Eicosanoids in Biological Samples Using Nano-flow Liquid Chromatography/Mass Spectrometry. *Analytical sciences : the international journal of the Japan Society for Analytical Chemistry* **2018,** *34* (2), 177-182. 10.2116/analsci.34.177.
29. Gowda, S. G. B.; Gao, Z. J.; Chen, Z.; Abe, T.; Hori, S.; Fukiya, S.; Ishizuka, S.; Yokota, A.; Chiba, H.; Hui, S. P., Untargeted Lipidomic Analysis of Plasma from High-fat Diet-induced Obese Rats Using UHPLC-Linear Trap Quadrupole-Orbitrap MS. *Analytical sciences : the international journal of the Japan Society for Analytical Chemistry* **2020,** *36* (7), 821-828. 10.2116/analsci.19P442.
30. Chiang, J. Y., Bile acid metabolism and signaling. *Comprehensive Physiology* **2013,** *3* (3), 1191-212. 10.1002/cphy.c120023.

31. Li, T.; Apte, U., Bile Acid Metabolism and Signaling in Cholestasis, Inflammation, and Cancer. *Advances in pharmacology (San Diego, Calif.)* **2015,** *74*, 263-302. 10.1016/bs.apha.2015.04.003.
32. Sun, W.; Zhang, D.; Wang, Z.; Sun, J.; Xu, B.; Chen, Y.; Ding, L.; Huang, X.; Lv, X.; Lu, J.; Bi, Y.; Xu, Q., Insulin Resistance is Associated With Total Bile Acid Level in Type 2 Diabetic and Nondiabetic Population: A Cross-Sectional Study. *Medicine* **2016,** *95* (10), e2778. 10.1097/MD.0000000000002778.
33. Zhao, X.; Peter, A.; Fritsche, J.; Elcnerova, M.; Fritsche, A.; Häring, H. U.; Schleicher, E. D.; Xu, G.; Lehmann, R., Changes of the plasma metabolome during an oral glucose tolerance test: is there more than glucose to look at? *American journal of physiology. Endocrinology and metabolism* **2009,** *296* (2), E384-93. 10.1152/ajpendo.90748.2008.
34. Lopaschuk, G. D., Fatty Acid Oxidation and Its Relation with Insulin Resistance and Associated Disorders. *Annals of nutrition & metabolism* **2016,** *68 Suppl 3*, 15-20. 10.1159/000448357.
35. Tangvarasittichai, S., Oxidative stress, insulin resistance, dyslipidemia and type 2 diabetes mellitus. *World journal of diabetes* **2015,** *6* (3), 456-80. 10.4239/wjd.v6.i3.456.
36. Moloney, F.; Yeow, T. P.; Mullen, A.; Nolan, J. J.; Roche, H. M., Conjugated linoleic acid supplementation, insulin sensitivity, and lipoprotein metabolism in patients with type 2 diabetes mellitus. *The American journal of clinical nutrition* **2004,** *80* (4), 887-95. 10.1093/ajcn/80.4.887.
37. Satapati, S.; Sunny, N. E.; Kucejova, B.; Fu, X.; He, T. T.; Méndez-Lucas, A.; Shelton, J. M.; Perales, J. C.; Browning, J. D.; Burgess, S. C., Elevated TCA cycle function in the pathology of diet-induced hepatic insulin resistance and fatty liver. *Journal of lipid research* **2012,** *53* (6), 1080-92. 10.1194/jlr.M023382.
38. Na, Z.; Jiang, H.; Meng, Y.; Song, J.; Feng, D.; Fang, Y.; Shi, B.; Li, D., Association of galactose and insulin resistance in polycystic ovary syndrome: A case-control study. *EClinicalMedicine* **2022,** *47*, 101379. 10.1016/j.eclinm.2022.101379.
39. Bo-Htay, C.; Shwe, T.; Higgins, L.; Palee, S.; Shinlapawittayatorn, K.; Chattipakorn, S. C.; Chattipakorn, N., Aging induced by D-galactose aggravates cardiac dysfunction via exacerbating mitochondrial dysfunction in obese insulin-resistant rats. *GeroScience* **2020,** *42* (1), 233-249. 10.1007/s11357-019-00132-9.
40. Hossain, P.; Kawar, B.; El Nahas, M., Obesity and diabetes in the developing world--a growing challenge. *The New England journal of medicine* **2007,** *356* (3), 213-5. 10.1056/NEJMp068177.
41. Chaurasia, B.; Summers, S. A., Ceramides - Lipotoxic Inducers of Metabolic Disorders. *Trends in endocrinology and metabolism: TEM* **2015,** *26* (10), 538-550. 10.1016/j.tem.2015.07.006.
42. Schubert, K. M.; Scheid, M. P.; Duronio, V., Ceramide inhibits protein kinase B/Akt by promoting dephosphorylation of serine 473. *The Journal of biological chemistry* **2000,** *275* (18), 13330-5. 10.1074/jbc.275.18.13330.
43. Wang, Y. M.; Seibenhener, M. L.; Vandenplas, M. L.; Wooten, M. W., Atypical PKC zeta is activated by ceramide, resulting in coactivation of NF-kappaB/JNK kinase and cell survival. *Journal of neuroscience research* **1999,** *55* (3), 293-302. 10.1002/(SICI)1097-4547(19990201)55:3<293::AID-JNR4>3.0.CO;2-9.
44. Amati, F.; Dubé, J. J.; Alvarez-Carnero, E.; Edreira, M. M.; Chomentowski, P.; Coen, P. M.; Switzer, G. E.; Bickel, P. E.; Stefanovic-Racic, M.; Toledo, F. G.; Goodpaster, B. H., Skeletal muscle triglycerides, diacylglycerols, and ceramides in insulin resistance: another paradox in endurance-trained athletes? *Diabetes* **2011,** *60* (10), 2588-97. 10.2337/db10-1221.

45. de la Maza, M. P.; Rodriguez, J. M.; Hirsch, S.; Leiva, L.; Barrera, G.; Bunout, D., Skeletal muscle ceramide species in men with abdominal obesity. *The journal of nutrition, health & aging* **2015,** *19* (4), 389-96. 10.1007/s12603-014-0548-7.
46. Kolak, M.; Westerbacka, J.; Velagapudi, V. R.; Wågsäter, D.; Yetukuri, L.; Makkonen, J.; Rissanen, A.; Häkkinen, A. M.; Lindell, M.; Bergholm, R.; Hamsten, A.; Eriksson, P.; Fisher, R. M.; Oresic, M.; Yki-Järvinen, H., Adipose tissue inflammation and increased ceramide content characterize subjects with high liver fat content independent of obesity. *Diabetes* **2007,** *56* (8), 1960-8. 10.2337/db07-0111.
47. Nokhoijav, E.; Guba, A.; Kumar, A.; Kunkli, B.; Kalló, G.; Káplár, M.; Somodi, S.; Garai, I.; Csutak, A.; Tóth, N.; Emri, M.; Tőzsér, J.; Csősz, É., Metabolomic Analysis of Serum and Tear Samples from Patients with Obesity and Type 2 Diabetes Mellitus. *International journal of molecular sciences* **2022,** *23* (9). 10.3390/ijms23094534.
48. Szczerbinski, L.; Wojciechowska, G.; Olichwier, A.; Taylor, M. A.; Puchta, U.; Konopka, P.; Paszko, A.; Citko, A.; Goscik, J.; Fiehn, O.; Fan, S.; Wasilewska, A.; Taranta-Janusz, K.; Kretowski, A., Untargeted Metabolomics Analysis of the Serum Metabolic Signature of Childhood Obesity. *Nutrients* **2022,** *14* (1). 10.3390/nu14010214.
49. Duft, R. G.; Castro, A.; Bonfante, I. L. P.; Lopes, W. A.; da Silva, L. R.; Chacon-Mikahil, M. P. T.; Leite, N.; Cavaglieri, C. R., Altered metabolomic profiling of overweight and obese adolescents after combined training is associated with reduced insulin resistance. *Scientific reports* **2020,** *10* (1), 16880. 10.1038/s41598-020-73943-y.

Distinct metabolomic profiling of serum samples from high fat diet-induced insulin resistant mice

Manendra Singh Tomar [a], Aditya Sharma[b], Fabrizio Araniti [c], Ankit Pateriya [a], Ashutosh Shrivastava [a*], Akhilesh Kumar Tamrakar [b*]

HFD-induced IR mice exhibit altered metabolomic pattern upon GC-MS analysis. The metabolites of the primary bile acid biosynthesis and linoleic acid metabolism are up accumulated; whereas metabolites of Pentose and glucuronate interconversions, and TCA cycle are down accumulated upon development of HFD-induced IR.

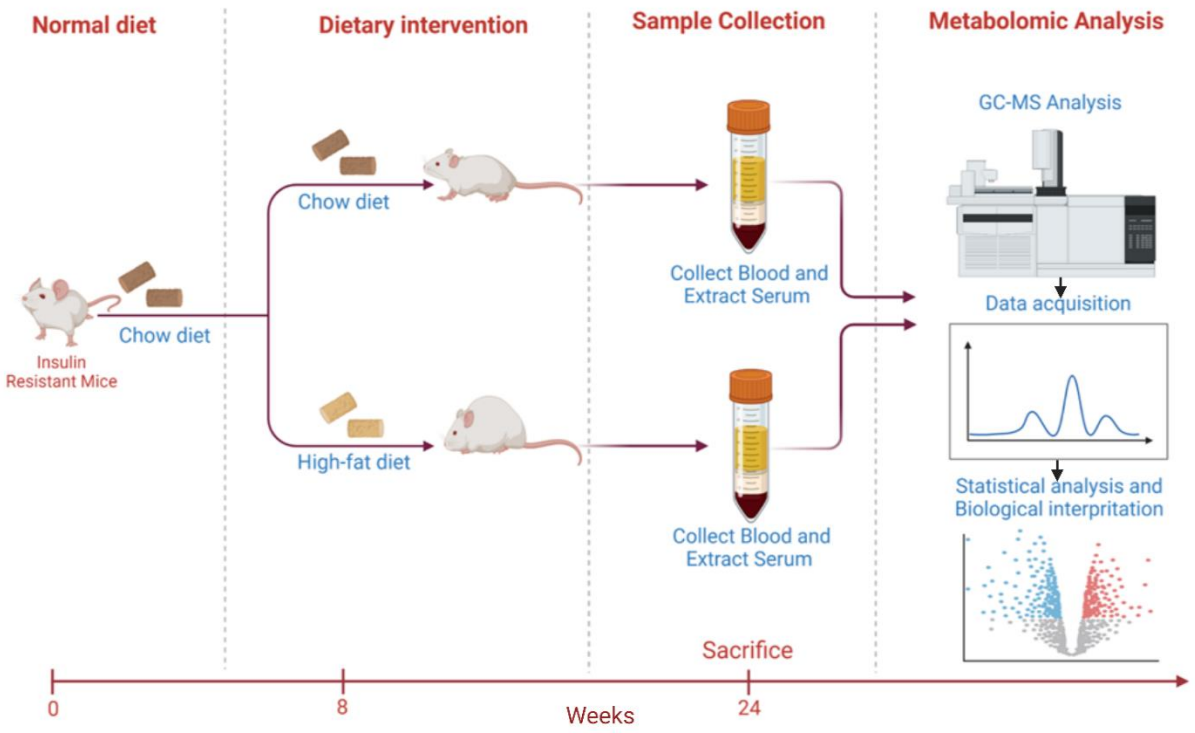

For Table of content use only